Chapter 2

Instrumentation and Analysis Techniques

2.1 Introduction

The rich astrophysical environment offered by the Magellanic Clouds, and the fact that they are the two nearest galaxies to our own, means that they provide one of the driving forces for building new and improved instrumentation in the southern hemisphere. The Clouds have been one of the principal observational targets of both the University of Sydney's Molonglo Observatory Synthesis Telescope (MOST) and the Australia Telescope Compact Array (ATCA) which is operated as a National Facility by the CSIRO. In this chapter the properties of these instruments are discussed, as are the various analysis techniques which are used to reduce data from these telescopes.

2.2 The Molonglo Observatory Synthesis Telescope

The MOST was commissioned in 1981 after an extensive upgrade programme to convert the 408 MHz Molonglo Cross from a transit instrument to an Earth-rotation aperture synthesis telescope operating at the higher (fixed) frequency of 843 MHz with a bandwidth of 3 MHz. The Cross consisted of two long, narrow, orthogonal antenna elements and this configuration formed instantaneously a narrow "pencil-beam" response where the two orthogonal fan-beam patterns intersect on the sky. The MOST utilized the existing east-west "arm" of the Molonglo Cross, which was mechanically tiltable in the north-south direction and electrically phased to point in the east-west direction, to provide synthesized images of far greater sensitivity and improved angular resolution. Two photographs of the MOST are reproduced in Figure 2.1.

The MOST consists of two collinear cylindrical parabolic reflectors each 778 m in length and approximately 11.6 m wide. The two arms are separated by a central gap of 15 m. At the focus of each reflector there are a series of rectangular waveguides which run the full length of each arm. The 843 MHz signal is received by 7744 helical ring elements (which receive right circular polarization – as defined by the IEEE) spaced

Figure 2.1: Two images of the Molonglo Observatory Synthesis Telescope. The top image was taken from the eastern end of the instrument at sunset and the bottom image was taken from the centre of the MOST looking towards the east as a storm approached. Both pictures were taken by the author.

along the waveguide at intervals of approximately half a wavelength. Two waveguides form what is known as a module (of length 8.84 m), and two modules a bay. There are 44 bays on each arm. The ring elements are differentially rotated by a mechanical gear train to set up a phase gradient along each module, thus steering the module beam in the east-west direction. The signal from each bay (i.e. two adjacent modules) is brought via cable to a mixer where the nominal 416 MHz local oscillator is doubled and mixed with the incoming 843 MHz signal. This forms the intermediate frequency (IF) signal, with a bandwidth of 3 MHz, at 11 MHz which is then fed to a multi-stage IF amplifier. These electronics are located along the antenna, one per bay. The IF signals from each bay are then brought back to the control room by equal-length cables, where amongst other processing, delay corrections are performed.

2.2.1 A Radio Schmidt

In many ways the MOST complements the higher-resolution and more frequency-agile aperture synthesis instruments (such as the ATCA) by being able to produce high quality, wide-field images in a single 12-hour observation. The "dirty" image from the MOST often requires no further data processing before astrophysical analysis can be undertaken. If higher-fidelity images are required, all that is usually necessary is the application of a standard Högbom CLEAN. The main effect of this is to decrease the amplitude of the first negative sidelobe which initially has an amplitude of around 10%.

The availability of good images in real-time, along with the fact that the MOST has good sensitivity to extended regions of low surface brightness, adequate resolution with a synthesized beam of about $43'' \times 43''\,\mathrm{cosec}\,|\delta|$ (where δ is the declination of the field centre) and a relatively large field size (up to $70' \times 70'\,\mathrm{cosec}\,|\delta|$), make the MOST a valuable large-field survey instrument. As a result of these features, the MOST has often been referred to as a "Radio Schmidt" telescope, playing an analogous role in radio astronomy to that played in optical astronomy by the UK Schmidt Telescope which neatly complements the Anglo-Australian Telescope. Observations with the MOST often form the basis of observing proposals for other instruments and are often used to provide radio "finding-charts" for higher-resolution studies. The characteristics outlined above suggest that the MOST is also an ideal instrument to carry out large and complete surveys of important regions of the southern sky and in particular the MOST survey of the Magellanic Clouds.

2.2.2 Some Special Characteristics of the MOST

Correlation and Beam-Formation

Unlike most other aperture synthesis telescopes, the MOST does not have the usual (XF or FX) correlator. Rather, it uses a resistor matrix to form appropriately weighted sine and cosine components which are combined to form total-power fan beams in real time. Corresponding fan beams from each "arm" are multiplied together and synchronously detected to form a set of 64 "hardware beams" spaced at $11''$ intervals. The same

fan beams can be added to form a corresponding set of total-power fan beams (with a corresponding $\sqrt{2}$ increase in sensitivity) which can be used for other experiments, either in their own right (such as for pulsar observations) where the stability obtained with a multiplying interferometer is not required, or for other observations which can be run in the background during normal synthesis observations. One such use of the total-power beams is the Molonglo Observatory Transient Event Recorder (MOTER) which is described in detail by Large et al. (1984). This piggy-back instrument searches for impulsive events over a range of timescales and has been used in the study of short-timescale astrophysics (Amy 1988; Amy, Large & Vaughan 1989). The MOTER detects many pulsars, and these can be used to calibrate the instrument.

The principal observing mode of the MOST is to operate as an Earth-rotation aperture synthesis telescope producing a high quality image over a period of 12 hours. The MOST survey of the Small and Large Magellanic Clouds was performed using this full-synthesis mode of operation. The continuous nature of the telescope (apart from the 15 m gap between the east and west arms) means that the common problem of missing spacings in interferometer data is somewhat lessened. However, there are other factors which degrade image quality and these are discussed later.

Another powerful MOST observing mode is known as "CUTS". Over a twelve-hour period, ten or more sources at different telescope pointings are observed for a few minutes each hour, ensuring that each source has been sampled over a large range of hour angles. This mode is typically used for relatively strong sources and is especially suited to imaging sources having a simple morphology, where a large number of sources need to be imaged over a relatively short observing session. Unfortunately it leads to increased wear on the mechanical components of the telescope, particularly due to the increase in the amount of slewing associated with the mechanical rotation of the ring elements.

Calibration

The calibration of complex visibility data obtained by "normal" Earth-rotation synthesis telescopes is an area of on-going research. Much of the work centres around the application of specialized calibration methods to the correlated complex visibilities, specified by their (u, v, w)-coordinates. A typical observing programme at the ATCA, for example, involves the observation of a secondary calibration source (particularly for phase calibration) for a few minutes every hour or so (the duty-cycle and integration time depending on such factors as observing frequency, atmospheric conditions and type of observing programme). At some stage during the observations a primary calibrator would also be observed to set the amplitude scale and (optionally) a polarization calibrator may also be observed. The bandpass can also be calibrated from a suitably long observation of the primary calibrator which is especially important in the case of spectral-line observations.

For the MOST, the resistor matrix performs a real time Fourier transform, which differs significantly from correlator-based synthesis instruments and hence requires alternative calibration methods. Typically, a small cluster of MOST calibrator sources

(typically four or five) is observed at the start and end of the 12 hour synthesis observation (usually a different cluster of sources is used at the end of the observations). This calibration strategy has the advantage that the target field is observed over the full range of hour angles, whereas, a typical ATCA observation of a single field will be interrupted with short observations of a secondary calibration source every 30-60 minutes. The MOST calibration sources are observed using an observing mode called SCAN where the telescope is scanned through the nominal source position five times per source. A fit to the resulting data determines three parameters known as *gain*, *offset* and *phase*. The data from all the SCAN sources (optionally excluding those which seem anomalous) are then averaged to form a global mean for each of the three parameters which can then be applied to the synthesis observation. The *gain* parameter provides the amplitude calibration for the synthesized map and is applied by a simple scaling of the data. The *offset* parameter is a measure of the offset of the peak of the fit from the nominal position of the source. The *phase* parameter is a measure of the asymmetry of the fit to the beamshape.

Another feature of the MOST requiring calibration is the variation in telescope gain as the source is tracked from east to west throughout the observation. The effect is believed to result from interference of the incoming ray with rays reflected from the feed line. The relevant angle, measured from the meridian, is the *Meridian Distance* (or MD) which is related to hour-angle (for an ideal east-west telescope) through the relation $\sin(\mathrm{MD}) = \cos\delta \times \sin(\mathrm{HA})$. To correct this quasi-sinusoidal variation in telescope gain, an *MD-gain* or *East-West Gain Function* is applied to the data during image formation (which is discussed in detail later). As can be seen from the form of the gain curve shown in Figure 2.2, the gain dependence is more critical for more northerly sources as the telescope must track the source over a larger range of MD. At the declination of the Magellanic Clouds, the Meridian Distance does not exceed $\pm 25^\circ$ which means that any errors in the MD gain function have less of an effect than it would, for example, in a synthesis of the Galactic Centre region. A number of determinations of the MD-gain functions have been performed at different times, in order to better characterize this gain variation. A detailed study by Burgess (1989) has provided the gain function shown in Figure 2.2.

Another effect that is particularly important for large-field and survey images is the variation of gain over the primary beam of the individual telescope modules. For an array such as the ATCA, this attenuation depends on a circularly symmetric function of λ/D, where λ is the observing wavelength and D is the diameter of the dish. The situation is more complex and less well-understood for the MOST, where the cylindrical antenna elements (approximately 17.7 m $\times$ 11.6 m) lead to a broad, quasi-elliptical antenna pattern. The correction made to much of the Magellanic Cloud survey data has been determined empirically (Reynolds 1985). This has proved to be adequate for much of the Magellanic Cloud survey as there are a significant number of overlapping fields and therefore only the inner portion of each $70'$ field is used.

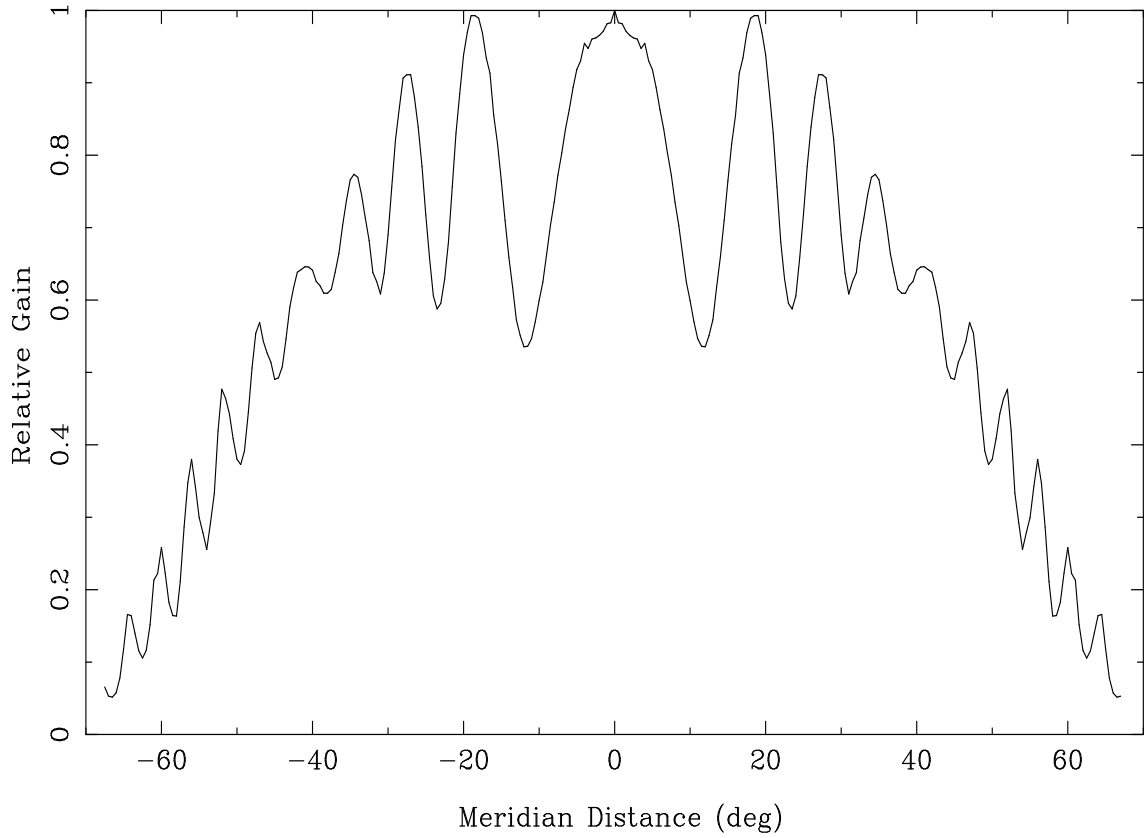

Figure 2.2: The East-West response of the MOST in the form of a function that is applied to the data during map formation. Note that the function is symmetric about MD = 0°. This particular curve was determined by Ann Burgess as part of her Physics IV project in 1989.

Imaging

The basic technique used for the formation of images is back projection (Crawford 1983). This method, where the beam responses are projected onto a two-dimensional representation of the sky brightness distribution, is similar to that used in medical imaging (e.g. CT scanning). Full hour-angle coverage is achieved by Earth-rotation aperture synthesis over a period of 12 hours. For the MOST, a data sample is recorded to magnetic disk every 24 seconds. Each sample contains a header followed by the responses of each fan beam as a (scaled) integer from the output of the analogue-to-digital converters. Depending on the field size observed ($23' \times 23'$ cosec $|\delta|$, $46' \times 46'$ cosec $|\delta|$ or $70' \times 70'$ cosec $|\delta|$) the number of beams recorded is either 128, 256 or 384 respectively and is obtained by time multiplexing the basic set of 64 fan beams every 2 seconds. The sample header contains parameters such as telescope error flags, date, time, temperature, right ascension, declination and other parameters which can be used during the data reduction.

The almost complete sampling of spatial frequencies means that high quality images result from this process. The back projection is performed in real time by the telescope's computer and a "dirty" image is typically available a few minutes after the completion of the observation. This image is available in the form of a contour plot or ruled-surface image, but has not yet had the SCAN calibration applied to it.

Deconvolution

Although it is possible to use the raw images for scientific purposes, it is usually desirable to re-synthesize (i.e. re-image) the data, applying the results from the SCAN calibration and removing any bad samples (due to interference or telescope malfunction). After a new "dirty" image is synthesized, a simple deconvolution in the form of the CLEAN algorithm is usually applied to produce the final high-quality image.

Imaging and calibration are performed using special-purpose software as none of the standard packages such as $\mathcal{AIPS}$ are suited to the unique calibration and imaging methods required for the MOST. The software used for much of the data presented in this thesis is known as $\mathcal{MSYN}$ and was originally developed by Dr J.E. Reynolds (Reynolds 1985). Since its development, this software has been extensively restructured, modified and enhanced (see, for example, Amy et al. 1991). In particular, synthesis in the J2000 equinox has been added together with routines to output to disk the resulting "dirty-map" and synthesized beam as FITS images. This facility allows standard astronomical software packages to be used to display, deconvolve and analyze the data. This approach utilizes the strengths and consistency of the various standard software packages.

The main software package used is $\mathcal{AIPS}$ which is widely available at many astronomical research institutions, and includes a full suite of tasks for analysis and display of the "dirty" image, the beam and the deconvolved image. MOST data can be deconvolved by loading both the "dirty-map" and "dirty-beam" into $\mathcal{AIPS}$ (as standard FITS images). The data can then be CLEANed using, for example, the task `APCLN`

which uses a modified algorithm (Clark 1980) in which many CLEAN components are subtracted in a single operation, or `HBCLN` which uses the more traditional Högbom CLEAN developed in the early 1970s. A higher CLEAN loop-gain can be used than is the norm for typical interferometer data because of the reasonably complete spatial frequency coverage of the MOST. Loop-gains of $0.25 - 0.3$ or even higher can be routinely used for MOST data, compared to the lower values (~ 0.1) typically used for ATCA data. If the beam has the same linear dimensions as the "dirty" map, only the centre quarter of the image can be fully CLEANed. To overcome these limitations $\mathcal{MSYN}$ can be used to make a double-sized beam (in linear dimensions) so the entire image can be deconvolved. A fully synthesized and calibrated "dirty" image and the corresponding deconvolved image of the MOST field 0104–724 is shown in Figure 2.3. This is the same data that were used in the study of the SMC SNR 1E 0102.2–7219 discussed in Chapter 6.

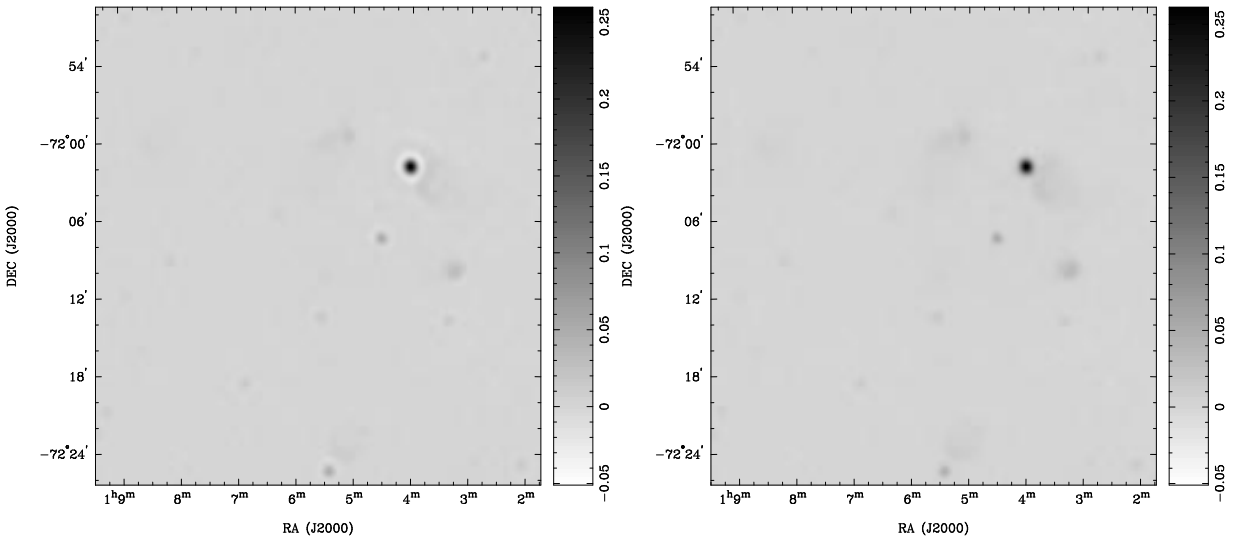

Figure 2.3: The "dirty" (left) and CLEANed (right) MOST images of the Small Magellanic Cloud field 0104–724. This was synthesized using $\mathcal{MSYN}$ with the appropriate gain, phase and offset parameters applied. The deconvolved image was obtained by using the $\mathcal{AIPS}$ task `APCLN`. Note the high quality of the "dirty" image. The strongest source in this field is the oxygen-rich SNR 1E 0102.2–7219 which is analyzed in detail in Chapter 6. The wedge to the right of each image gives an indication of the transfer function.

Problems Unique to the MOST

The MOST differs from other Earth-rotation aperture synthesis interferometers in several ways. These differences present some unique problems when it comes to improving image quality for later analysis.

The fact that the MOST forms fan beams in real time has the drawback that the traditional *visibility* information is not available during data reduction. For instruments

such as the Australia Telescope this information enables the data to be edited on a "per-baseline" or "per-channel" basis.

The calibration procedure actually used for the MOST is not ideal in that it relies on the stability of both the instrument and the atmosphere over the 12-hour observing period. Furthermore, calibration data are often recorded around sunset and/or sunrise when it is likely that the atmosphere is less than ideal and the sun lies close to the endfire direction of the feed lines. The calibration data obtained may therefore *not* be representative of the conditions during the major part of the synthesis observation. At the observing frequency of the MOST (843 MHz) it is likely that ionospheric conditions cause much of the phase instability that is sometimes observed. Atmospheric conditions become increasingly important as the observing frequency increases. For example, the phase at the ATCA has been seen to go through a full turn (i.e. 360°) in less than 20 minutes when observing at 8.4 GHz with a baseline of 6 km (Norris 1993). Tropospheric conditions are also important at 843 MHz and are believed to explain a number of features in MOST images. For the MOST, more accurate source positions can usually be obtained (providing the sources are relatively strong) using the "CUTS" mode of observing, which enables calibration sources to be observed as often as desired, typically once per hour.

Grating Responses

An east-west synthesis telescope consisting of regularly spaced antenna elements (such as the MOST) produces a grating response which is manifested in the resulting images as elliptical rings about each source with a diameter related to the spacing of the individual antenna elements. It is desirable that these occur as far as possible from the source to avoid degradation of the resulting image by these grating responses.

In the case of the MOST, the principal grating response occurs at an offset of 1.15 degrees and is caused by the regular spacing of the modules (at 8.84 m) and the bays (17.7 m). The mechanical phasing by the differential rotation of the individual helical ring elements and the beam formation leads to a more complicated grating response than in conventional east-west arrays. Each bay is phased correctly for the position of the field centre by the differential rotation of the antenna elements. This is analogous to the beam formed by an individual antenna in an array such as the ATCA. However, other instantaneous fan beams are formed by various combinations of phase and delay of the signals from the bays, and these exhibit an increasing periodic phase error the further the fan beam is offset from the field centre. The fan beam at the field centre has (ideally) the correct phase and delay and does not excite a grating response.

MOST surveys are typically made with the largest synthesized field that is available ($70' \times 70' \operatorname{cosec} |\delta|$) to maximize coverage and the speed of the survey. The grating responses are at their worst in these large-field images, since the set of 64 fan beams are significantly offset relative to the primary beam which is fixed at the field centre. In principle, the primary beam of each bay could be moved synchronously with the set of fan beams, but the speed of the multiplexing required prohibits this technique which would require the mechanical rotation of the antenna elements (to change the phase

gradient) every 2 s. An alternative solution has been adopted, inserting a 60° phase shift into the appropriate module of each bay when the fan beams are in one of the offset positions (Amy & Large 1990; 1992). The effect of this is to move the primary beam of each bay to the position of the set of offset beams. Although not perfect, the grating response amplitude is reduced to a maximum of 12% of the uncorrected value, significantly improving the quality of 70′ field images, including images from the Galactic Survey and the Magellanic Cloud Survey. This work was used as the basis for a major upgrade to the MOST which involved the installation of new low-noise preamplifiers, quad phase-shifters, mixers and IF sections and updated communication and control systems (Large et al. 1994).

Additional information on the MOST and its design and operation are given in Mills (1981) and Robertson (1991).

2.3 The Australia Telescope

The Australia Telescope project was funded by the Australian Federal Government in 1983 as a Bicentennial Project and, as part of the bicentenary celebrations, it was officially opened by the Prime Minister on 2 September 1988. One of the key factors in the success of the bid for funding the project was that it would have over 80% Australian content. It was argued that the project would enable the development of new design and fabrication techniques that could be used in other areas of Australian industry and this claim has been well-justified. The project was managed by the CSIRO Division of Radiophysics, and in 1989, a new Division of CSIRO called the Australia Telescope National Facility (ATNF) was formed. The ATNF has responsibility for the operation and future enhancements of the Australia Telescope.

2.3.1 Why was it Built?

As with any new astronomical instrument, there were scientific driving forces for the construction of the AT. Three main reasons for building the instrument emphasized the strengths of the location of Australia in the Southern Hemisphere: they are the accessibility of the Galactic Centre, Centaurus-A and the Small and Large Magellanic Clouds.

It was becoming clear in the late 1970s that Australia needed a more powerful radio-telescope. At the time, the Mills' Cross was being converted to the MOST and the only other synthesis instrument in Australia (and indeed the Southern Hemisphere) at the time was the Fleurs Synthesis Telescope operated by the Department of Electrical Engineering at the University of Sydney. Fleurs operated at the fixed-frequency of 1415 MHz, and the MOST was also a fixed frequency instrument operating at 843 MHz. Furthermore the MOST was only capable of receiving right-circular polarization. Thus there was no frequency-agile synthesis instrument in Australia, nor was there any capability for polarimetry studies or for producing spectral-line synthesis images.

The technical aims of the AT included provision for operation over a wide range of

frequencies and an ability to perform bandwidth synthesis in each of the designated frequency bands. This is important to maximize the spatial frequency coverage with a modest number of baselines. The ability to observe at two frequencies simultaneously, retaining full polarization information, was another important design issue. This feature was used in the study of SNR 1E 0102.2–7219 discussed later in this thesis. In addition, the AT has the capability to observe in various spectral line modes and to re-configure the receiving systems, local oscillators and correlator quickly and easily. One of the more interesting design features of the AT is that IF signals are digitized at each antenna and transmitted back to the delay units and correlator on optical fibre.

2.3.2 What Is and Where Is the Australia Telescope?

The AT consists of the Compact Array (ATCA) at Narrabri approximately 600 km north-west of Sydney, a single 22 m antenna near Coonabarabran (called "Mopra") located about 120 km south of Narrabri and the pre-existing 64 m Parkes Radio Telescope some 400 km to the west of Sydney. Pictures of the ATCA and the Parkes Radio Telescope are shown in Figure 2.4.

The ATCA consists of six 22 m antennas over a 6 km east-west baseline. Five of these antennas are located on a 3 km track with 35 stations. The 5 antennas can be moved to various stations to obtain configurations matching the spatial frequency coverage to the requirements of the observing programme. The sixth antenna is located on an 80 m section of track with two stations 3 km distant from the 3 km array. The antenna surfaces consist of solid inner panels to a diameter of 15 m and then perforated panels to the full 22 m diameter. This reduces wind loading while retaining a future mm-wave capability. The inner surface was designed to be sufficiently accurate for observations up to 115 GHz.

Mopra, the seventh 22 m antenna, is located at a separate site near Siding-Springs Observatory, Coonabarabran. This site is close to the Anglo-Australian (optical) Telescope and other optical instrumentation from the Australian National University and the University of New South Wales. The Mopra antenna is of similar design to the six antennas which make up the Compact Array. However it is on a fixed base rather than a track, and was designed to provide better surface accuracy and better tracking, making it more suitable as a single-dish mm-wave instrument using the inner 15 m surface.

The final antenna comprising the Australia Telescope is the 64 m Parkes dish, constructed in the late 1950's/early 1960's. Although its primary mode of operation is as a stand-alone telescope, Parkes, Mopra and the ATCA have been successfully combined for Very Long Baseline Interferometry (VLBI) experiments. The Compact Array is able to operate in a "split-array" mode in which one antenna is controlled independently for VLBI, and the other five antennas are used for synthesis imaging observations.

Further details on the design and construction is given in Frater & Brooks (1992).

Figure 2.4: The top panel show an image of the Parkes 64 m antenna taken at sunset. The bottom panel shows five antennas of the Australia Telescope Compact Array at Narrabri in the compact 122 m array. Both pictures were taken by the author.

2.3.3 ATCA Observing Techniques

The ATCA has unique capabilities, and many of the observations reported here were among the first to exploit these as the telescope moved from construction to a full-service facility. Some of the issues considered here are: the availability of wide continuum bandwidth and bandwidth synthesis; simultaneous dual frequency operation; multi-frequency synthesis; spectral line operation; and "CUTS" observations.

Continuum Observations

Although the number of baselines of the ATCA are limited (to $6 \times 5/2 = 15$), the wide continuum observing bandwidth can assist to some extent in improving the (u, v)-coverage and sensitivity. The key factor in being able to achieve this is that the AT correlator uses a minimum of 32 frequency channels even when observing in so-called *continuum* mode. In this mode there are 32 (non-independent) channels spaced over the full 128 MHz bandwidth (assuming the use of 2-bit digitization – other options are 1-bit and 4-bit). By recording the separate channels, rather than averaging all the channels into a single (centre) frequency, the visibility data for each channel can be correctly gridded in the spatial frequency domain. This process is commonly referred to as bandwidth synthesis. The "band centre" point in the spatial frequency domain is thus effectively "expanded" to cover a range of spatial frequencies corresponding to the frequencies observed across the band. The technique is most powerful at lower observing frequencies where the fractional bandwidth is greatest. For example, in the 20 cm band the fractional bandwidth is almost 10% (using a 128 MHz bandwidth at a centre frequency of 1420 MHz).

The use of narrow continuum channels to grid correctly the visibility data also avoids "bandwidth smearing". If a wide continuum band is used, a point source offset from the phase centre of an observation will appear smeared in the radial direction from the phase centre. This can result in the observed amplitude being less than the true amplitude as a range of spatial frequencies have been represented (or approximated) by a single point in the (u, v)-plane. The ratio, A, of observed amplitude to true amplitude in a 4 MHz channel is given by:

$$A = 1 - r \times b/130$$

where r is the distance from the phase centre in arcmin and b is the baseline length in km. For sources close to the phase centre – and for observations at the higher frequencies (where the fractional bandwidth is relatively small) – this effect is negligible, but in other cases the extra analysis required for bandwidth synthesis can lead to scientifically richer results.

Simultaneous Dual Frequency Operation

The AT has the ability to operate at two separate frequencies simultaneously, recording the full bandwidth and a full set of Stokes parameters at each frequency. This is

made possible by the grouping of feed, receiver and associated backend electronics packages into a 20/13 cm package and a 6/3 cm package. Each of these packages has a single feedhorn covering a wide frequency range (typically a few GHz) and coupled into the appropriate receiver package. Providing the two desired frequencies lie within the range of these packages, the observing frequencies can be centred wherever the observing programme requires. For example in the 20/13 cm band it is possible to observe two 128 MHz bands in the 20 cm band, or to choose one in the 20 cm band and the other in the 13 cm band. On a longer timescale, say once every 15 minutes or so, it is possible to switch between the 20/13 cm package and the 6/3 cm package. This involves a mechanical rotation of the turret to bring the requested feedhorn/receiver package on axis. The turret rotation operation is now (since August 1993) controlled automatically by the observing programme with the feed selected according to the specified observing frequency. It is however impossible to observe simultaneously at one frequency in the 20/13 cm bands and the other in the 6/3 cm bands, because physically different feedhorn/receiver packages cover these frequency ranges.

The dual-frequency observing capabilities of the ATCA were used to great effect in the study of SNR 1E 0102.2–7219 discussed in Chapter 6. Two frequencies (generally 1472 MHz and 2368 MHz, then 4790 MHz and 8640 MHz) were observed in each observing run. This enabled the spectral index to be determined, the changes in morphology that occur over the observed frequency range to be studied, and the variation of polarized intensity with frequency to be established.

Multi-frequency Synthesis

The term multi-frequency synthesis is used to describe a technique whereby a set of distinct frequencies are observed over a short time interval to better sample the spatial frequency domain. The set of frequencies is chosen so as to maximize the (u, v)-coverage within a given band and a number of tools have been developed to determine this optimal set of frequencies. The variation of intensity with frequency may significantly affect the combined image and it is important to be aware of this when analysing the data. Techniques that can successfully compensate for the spectral variation do exist. None of the AT observations discussed in this thesis take advantage of the multi-frequency synthesis technique as most were made before the necessary analysis techniques were available.

Spectral-line Observing

One strength of the ATCA system design is its flexibility as a spectral-line instrument. The fact that the ATCA operates in spectral-line mode even during so-called "continuum" observations, although a little unconventional, enables individual frequency channels to be edited. This is useful when narrow-band interference is present in the data. If there was only a single continuum channel, such interference would probably require the entire baseline to be excised. However, with the ATCA only the affected channels need to be excised and the remainder of the data are retained. This saving has

been used on the short baselines of the SNR 1E 0102.2–7219 data, both at 1472 MHz and 2368 MHz, where strong but narrow-band interference was present during the observations.

True spectral-line observing involves much narrower bandwidths with many more channels across the band. As would be expected, there is a trade-off between bandwidth, number of channels, correlation time and time to output the data from the correlator to magnetic disk. The ATCA correlator control computer can be configured to allow for a subset of the full band to be written to disk, thus enabling the desired resolution to be observed but significantly reducing the volume of raw data. Bandpass stability is vitally important for spectral line observations and bandpass calibration is therefore also critical. Typically, bandpass calibration is achieved by a 20-30 minute observation of a strong calibration source; the primary flux calibrator being often used for this purpose.

ATCA "CUTS" Observing

The ATCA can be used for a mode of observing named after, and reminiscent of, the MOST "CUTS" observing mode. This mode departs from the original design goals of the ATCA, which were based on the premise that most observing programmes would require four configurations of about 12 hours per source to produce an image of quality suitable for subsequent analysis. However, both myself and Dr A.J. Turtle realized that by using a number of short "CUTS" the ATCA could be exploited to survey quickly a large number compact sources in the Magellanic Clouds.

The strategy we employed was to phase calibrate once per hour for about 4 minutes using a nearby secondary calibrator, and then spend about 5 minutes (including telescope drive time) per target source, cycling around the complete group of sources about once per hour. The key to the success of this technique (as with the MOST) is that each source is sampled at about 12 distinct hour angles over the range $-90^\circ <$ HA $< +90^\circ$. As the sources were all quite close to each other and to the secondary calibrator, the drive time was usually short, typically of the order of 30–45 seconds. As these observations were undertaken just after the ATCA was officially available for observing, the biggest problem experienced was the time taken for the sampler statistics to stabilize after each source change; typically 3–4 integration periods each of 10 s. Nonetheless, this proved a very successful and economical way of surveying a large number of sources (which had a relatively simple morphology) in only a few observing sessions. Without the "CUTS" observing technique it is unlikely that these surveys could have been completed.

2.3.4 Calibration and Polarimetry at the ATCA

An important consideration in the design of the ATCA was that it should have well-defined polarization characteristics over the large bandwidth provided by its corrugated feed horns. One of the aims of the multi-frequency ATCA observations of SNR 1E 0102.2–7219 presented in Chapter 6 was to exploit this capability to measure any

polarized emission. At the time of these observations, both the telescope hardware and data reduction techniques were still being developed. I therefore present an overview of the theory of polarization and its observation, and detail the steps followed to carry out full polarization calibration of these ATCA observations. The procedure has since been greatly simplified. ATCA polarization data obtained after November 1992 benefit from an accurate on-line determination of the XY-phase, and the necessary analysis techniques have now been standardized and refined.

Most large aperture-synthesis arrays (including the VLA) have circularly polarized feeds. The ATCA, however, has linear feeds located at the base of the wide-band feed horns. The decision to use linear feeds raised issues concerning the polarization calibration of ATCA data, and in particular, which software should be used to reduce the data. The most widely used data reduction package in radioastronomy is $\mathcal{AIPS}$, but the $\mathcal{AIPS}$ calibration routines are tailored to handle circularly-polarized data. An alternative package called $\mathcal{MIRIAD}$ (Sault et al. 1995) has therefore been adopted. This package has the advantage that it could be easily modified to support the linear feeds of the ATCA. It should be noted that the reduction of total intensity images can be done without special calibration routines. Thus when full polarimetric analysis is either not possible because of the limitations of the raw data, or is not required, ATCA data can be reduced using $\mathcal{AIPS}$. This is true of a significant fraction of ATCA data, including much of the data presented in this thesis which was obtained soon after the ATCA was commissioned.

It is usually convenient to describe a polarized radiation field in terms of a set of four parameters, I, Q, U and V commonly referred to as Stokes parameters (after Sir George Stokes who introduced this concept in 1852). In the case of the ATCA where the dual-polarization feeds measure two linear polarizations, referred to as X and Y, the four visibility functions (or correlations) that are available are $X \times X$, $Y \times Y$, $X \times Y$ and $Y \times X$; generally denoted XX, YY, XY and YX. In the simplest situation where only a total intensity (or Stokes I) image is required, we need only be concerned with the two "pure" linear components XX and YY as explained below. In this case, the complex gains of the two polarized signals can be calibrated using $\mathcal{AIPS}$ routines designed to handle circularly polarized data. The technique used is to change the data header (typically as the data are loaded) to label XX as RR and YY as LL (where RR is $R \times R$ and LL is $L \times L$ – the two hands of circular polarization). In practice this is easily achieved with the AT specific $\mathcal{AIPS}$ task `ATLOD`.

Stokes Parameters

An overview of the relationship between Stokes parameters, the incident electric field and the overall calibration procedure in the context of radioastronomical data is useful at this point.

If E_x and E_y are the components of the electric field resolved into two perpendicular axes normal to the direction of propagation from a point source, we can write

$$E_x = e_x(t)\,\cos[2\pi\nu t + \delta_x(t)], \quad \text{and} \tag{2.1}$$

$$E_y = e_y(t)\,\cos[2\pi\nu t + \delta_y(t)]. \tag{2.2}$$

where e_x and e_y are the components of the complex amplitude of the electric field and δ is a time-variable phase term. The four Stokes parameters are defined as:

$$\begin{aligned} I &= \left\langle e_x^2(t)\right\rangle + \left\langle e_y^2(t)\right\rangle, \\ Q &= \left\langle e_x^2(t)\right\rangle - \left\langle e_y^2(t)\right\rangle, \\ U &= 2\left\langle e_x(t)e_y(t)\cos[\delta_x(t)-\delta_y(t)]\right\rangle, \quad \text{and} \\ V &= 2\left\langle e_x(t)e_y(t)\sin[\delta_x(t)-\delta_y(t)]\right\rangle, \end{aligned} \tag{2.3}$$

where the angle brackets indicate a time average. Here, I represents the total intensity, Q and U represent the linearly polarized component and V represents the circularly polarized component. These four parameters, together with the frequency, fully describe the polarization state of the incident radiation.

It is instructive to consider the difference between the expressions for the response of linearly-polarized and circularly-polarized feeds to a polarized wave as expressed in terms of the Stokes parameters. In both cases, the instantaneous response is a linear combination of two Stokes parameters. For (ideal) circular feeds

$$\begin{aligned} RR &= I + V, \\ LL &= I - V, \\ RL &= U - iQ, \quad \text{and} \\ LR &= U + iQ. \end{aligned}$$

Since the sources used to calibrate the (complex) antenna gains are usually not circularly polarized, Stokes $V = 0$ and so does not contribute to the RR and LL visibilities. Thus, the RR and LL are a *direct* measure of Stokes I for sources for which we know the flux density and morphology (generally a point-source), and as such these visibilities can be used to determine the variation of antenna gain as a function of time. For ideal linear feeds

$$\begin{aligned} XX &= I + Q, \\ YY &= I - Q, \\ XY &= U + iV, \\ YX &= U - iV, \end{aligned}$$

where the X and Y feeds are at position angles of 0° and 90° respectively. It is important to realize that it is more difficult to calibrate a linear feed array than a circular

feed array. To calibrate linearly polarized feeds it is desirable to use sources with no linear polarization. Unfortunately, many cosmic sources are linearly polarized, albeit only by a few percent, and so the XX and YY visibilities do not provide independent measurements of the total intensity I.

Further factors must be taken into account before accurate Stokes parameters can be determined. For an 'alt-az' telescope such as the ATCA, the feeds rotate with respect to the source throughout the observation. Thus the feed response varies with parallactic angle as a function of time, and the expressions for the set of four visibilities have to take account of this variation. In addition, the above treatment assumed that the feeds were ideal such that the x-component of the incident electric field is *only* received by the X-feed with the Y-feed recording zero signal from this component and vice-versa. In practice, the feeds are not ideal and so there are (complex) "leakage" terms which must be taken into account. Note that the XY-phase is the difference between the phase of the gains of each feed in *each* antenna. This is usually set to zero at the start of an observation. Thus to perform an accurate conversion from correlated visibilities into Stokes parameters, the complex antenna gains and the leakage terms must be determined. When the data are first loaded into $\mathcal{AIPS}$ using the `ATLOD` task and the option to convert to Stokes is selected, `ATLOD` assumes that the complex gains are equal and that the leakage terms are zero and therefore only makes a nominal conversion to Stokes parameters. This is generally adequate for total intensity imaging and was used for a number of the observing programmes discussed in this thesis.

All four Stokes parameters have units of flux density, and I is just the total intensity. The interpretation of Q, U and V as physical quantities is more obvious in terms of the combinations of these parameters to give m_l, the degree of linear polarization; m_c the fraction of circular polarization; m_t, the total polarization and ψ, the polarization angle expressed in terms of a position angle (increasing from north through east), as follows:

$$m_l = \frac{\sqrt{Q^2+U^2}}{I}, \tag{2.4}$$

$$m_c = \frac{V}{I}, \tag{2.5}$$

$$m_t = \frac{\sqrt{Q^2+U^2+V^2}}{I}, \quad \text{and} \tag{2.6}$$

$$\psi = \frac{1}{2}\arctan\left(\frac{U}{Q}\right), \qquad 0 \leq \psi \leq \pi. \tag{2.7}$$

The usual procedure which is followed is to make separate images corresponding to Stokes I, Q, U and V. These images can then be deconvolved (using, for example, the CLEAN algorithm) before combining to form polarized intensity and polarization angle images. The deconvolution is non-linear and must be carried out before the images are combined. Most software packages provide a task that manipulates the images according to the above equations. In $\mathcal{AIPS}$ the task used is `COMB` and in

MIRIAD the task is `impol`. Note that the polarized intensity image as determined from Equation 2.4 is positive, whereas the Q, U and V images may be positive or negative depending on the position angle of the polarized emission. A technique known as "de-biasing" is usually applied to the (positive definite) polarized intensity image. This is used to correct for the skewed distribution of pixel intensities at low signal-to-noise ratios which follow a Ricean distribution. A reasonably accurate estimate of the noise can be obtained from the Stokes V image, which should just be pure noise as most radio sources do not have any component of circular polarization. Thus the Stokes V image can also be used to assess the success or otherwise of editing and calibration, and to identify other instrument artifacts that could be difficult or impossible to detect when analyzing an image (e.g. I, Q or U) that contains flux.

A Stepwise Approach to Full Polarization Calibration

This methodology assumes that the array was correctly calibrated on-line, and that any necessary observing parameters were set. It is also assumed that the data were correctly loaded (taking account of the the XY-phase measurements and taking corrective action where necessary), any bad data have been expunged and that the multi-channel continuum data have been averaged into a single "Channel 0" dataset using *AIPS*. After each step the success of the calibration should be assessed by plotting and examining the visibility data against other observed and derived parameters, and corrective action taken if necessary.

1. Set the flux density of the chosen primary calibrator. For almost all the data presented in this thesis, the source B1934–638 was used as the primary calibrator.

2. Using the secondary calibrator determine the antenna gains, the instrumental polarization and the XY-phases for all antennas except the reference antenna. The instrumental polarization terms are also known as the "leakage" terms.

3. Copy the polarization leakage terms and the XY-phase difference tables to the short observation (typically about 10 minutes) of a known position-angle calibrator. The source 3C286 was used for the polarization observations presented in this thesis.

4. Determine the residual XY-phase difference, alignment and ellipticity of the X feed of the reference antenna using the known polarization calibrator.

5. Copy the new polarization leakage table from the position-angle calibrator to the primary calibrator and solve for the Stokes I flux of the primary calibrator.

6. Bootstrap the flux density of the secondary calibrator using the primary calibrator.

7. Interpolate the above calibration onto the program source.

2.4 Summary

Data analysis methods in radio astronomy are being continually developed and improved to cope with new observational techniques. The instrumentation and data analysis techniques described in this chapter are those which have been directly used to analyse the MOST and ATCA observations presented in this thesis.

The MOST has been significantly upgraded in the late-1990s, leveraging the earlier work on phase shifters, to enlarge the synthesized field size in order to undertake a complete survey of the southern sky at 843 MHz over the next 5–10 years. The Australia Telescope has embarked on significant hardware and software upgrades in order to operate at millimetre wavelengths. It is clear that both the MOST and ATCA will continue to complement each other as major radio astronomy facilities in the southern hemisphere.